



<http://researchspace.auckland.ac.nz>

ResearchSpace@Auckland

Copyright Statement

The digital copy of this thesis is protected by the Copyright Act 1994 (New Zealand).

This thesis may be consulted by you, provided you comply with the provisions of the Act and the following conditions of use:

- Any use you make of these documents or images must be for research or private study purposes only, and you may not make them available to any other person.
- Authors control the copyright of their thesis. You will recognise the author's right to be identified as the author of this thesis, and due acknowledgement will be made to the author where appropriate.
- You will obtain the author's permission before publishing any material from their thesis.

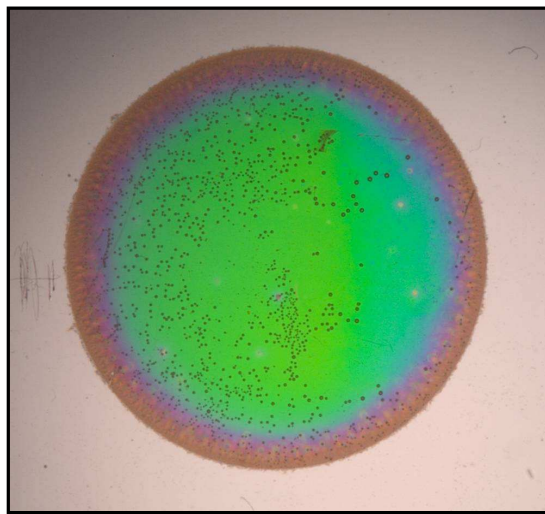
To request permissions please use the Feedback form on our webpage.

<http://researchspace.auckland.ac.nz/feedback>

General copyright and disclaimer

In addition to the above conditions, authors give their consent for the digital copy of their work to be used subject to the conditions specified on the Library Thesis Consent Form.

Development of Chemical Gradients across Porous Silicon Sensors



Corrina Thompson

A thesis submitted in fulfillment of the requirements for the degree of Doctor of
Philosophy

The University of Auckland, 2009

Abstract

This thesis investigated the formation of compositional gradients across 0.5 – 1 cm of porous silicon layers which had thicknesses of 2 – 10 μm . These compositional gradients were then characterised, and their potential use as vapour sensors was probed. Surface composition gradients have been reported on flat surfaces, but this is the first time that they have been reported on a three-dimensional material with controlled pore geometry.

Chemical gradients have been generated across the surface of porous silicon by performing electrochemical attachment of organohalides with an asymmetric electrode arrangement, and by chemical hydrosilylation of alkenes in the presence of a diffusion gradient of diazonium salts across the porous silicon surface. Samples with electrochemical gradients of methyl, pentyl acetate, and decyl and using chemical hydrosilylation with gradients of undecanoic acid and decyl groups. The latter four gradient-modified porous silicon types have been 'endcapped' with methyl groups to give improved stability and greater hydrophobicity. The pentyl acetate and undecanoic groups have been converted into pentanol and undecanoate groups respectively to increase the hydrophilicity of these porous silicon surfaces. The gradients have been characterised using two-dimensional FTIR microspectrophotometry and water contact angle measurements.

The interaction of these gradient porous silicon samples with ethanol, heptane, toluene and 2-hexanol vapours have been monitored either by UV-Vis reflectance spectroscopy at selected points across the surface or more globally using a digital camera. The undecanoate gradient porous silicon sample showed a large difference in optical response between the undecanoate end and the methyl end of the gradient when exposed to water vapour, showing that imposition of a chemical gradient can alter the sensing character of porous silicon in a controllable manner.

Acknowledgements

This research would not have been possible without the help and encouragement from the following people.

First and foremost, I would like to thank Dr Gordon Miskelly for always providing guidance, ideas and assistance. You have been a great mentor and supervisor who provided a fresh opinion and idea when required and kept me focussed on the research at hand.

I would also like to thank Prof. Mike Sailor at UCSD for providing guidance and hosting me while I was in San Diego and the Sailor group members especially Anne Ruminski for the lengthy and productive discussions.

To all the technical staff at the Auckland University Chemistry Department I thank you, especially Michel Nieuwoudt for providing assistance with FTIR measurements, Glenn Boyes who never became tired of my endless queries for chemicals and use of equipment, and the glass blowers Alistair Mead and Michael Wadsworth who never became tired of my endless queries about making custom glass equipment. I would also like to thank Catherine Hobbs and Colin Doyle in the Faculty of Engineering for assisting with SEM and XPS measurements.

To all the members of my group, present and past, John, Chu, Lim, Debbie, Hazel, Toyah, Peter, Gareth, Liz, Sarah, Marsilea and Grant (I know your not in our group but you're an honorary member) thanks for all the support.

A special thanks for John who listened to my complaining and stressing. You kept me going with your loving support and encouragement when things weren't going so well. Thank You.

And finally I would like to thank my family and friends for their encouragement and support.

Table of contents

Abstract	ii
Acknowledgements	iii
Table of contents	iv
List of figures	viii
List of tables	xix
Abbreviations	xxi
CHAPTER 1 INTRODUCTION	1
1.1 INTRODUCTION	2
1.2 REAL-TIME SENSING	2
1.3 POROUS SILICON	5
1.3.1 <i>Brief history of porous silicon</i>	5
1.3.2 <i>Formation of porous silicon</i>	6
1.3.2.1 Structure of porous silicon.....	9
1.3.2.2 Pore size gradients across porous silicon.....	11
1.3.3 <i>Modification of porous silicon</i>	11
1.3.3.1 Silicon oxygen bonds on porous silicon	11
Oxidation of porous silicon to form silicon oxides	11
Attachment of organic groups to porous silicon via silicon-oxygen bonds.....	13
1.3.3.2 Silicon-carbon bonds to porous silicon.....	14
Electrochemical modification of porous silicon	15
Hydrosilylation reactions	16
Other methods	19
1.3.3.3 Patterning.....	20
1.3.4 <i>Characterisation of porous silicon</i>	20
1.3.5 <i>Properties of porous silicon used in sensing applications</i>	23
1.3.5.1 Porous silicon sensors based on photoluminescence	26
1.3.5.2 Porous silicon sensors based on electrical properties	27
1.3.5.3 Porous silicon sensors based on optical reflectance.....	27
Porous silicon sensors based on complex optical structures.....	30
1.4 FORMATION OF CHEMICAL GRADIENTS	32
1.4.1 <i>Introduction</i>	32
1.4.2 <i>Techniques for gradient formation</i>	33
1.4.2.1 Gradient formation by lithography	33
1.4.2.2 Gradient formation by chemical diffusion.....	34
1.4.2.3 Gradient formation by non-diffusive concentration gradients	36
1.4.2.4 Gradient formation by gradual immersion or removal from a liquid medium.....	37
1.4.2.5 Gradient formation by electrochemical methods	38
1.4.2.6 Gradient formation by other methods.....	38
1.4.3 <i>Possible methods for gradient modification of porous silicon</i>	39
1.5 AIMS OF THIS RESEARCH.....	39
CHAPTER 2 EXPERIMENTAL	41
2.1 MATERIALS.....	42
2.1.1 <i>Solvents</i>	42
2.1.2 <i>Specialised Chemicals</i>	42
2.1.3 <i>Silicon wafers</i>	43
2.2 SYNTHESSES	43
2.2.1 <i>Nuclear Magnetic Resonance</i>	43
2.2.2 <i>Synthesis of Diazonium Salts</i>	43
2.2.2.1 Synthesis of 4-bromobenzenediazonium tetrafluoroborate (BBD)	43

2.2.2.2	Synthesis of 3,4,5-trifluorobenzenediazonium tetrafluoroborate (FBD).....	44
2.3	POROUS SILICON PREPARATION.....	45
2.3.1	<i>Hydrofluoric acid safety</i>	45
2.3.2	<i>Instruments</i>	45
2.3.2.1	Potentiostat/Galvanostat	45
2.3.2.2	Function Generator	46
2.3.3	<i>Electrochemical cell setup for porous silicon preparation</i>	46
2.3.4	<i>Principal porous silicon etching method</i>	47
2.3.4.1	Fabry-Perot layer etching method.....	47
2.3.4.2	'Uniform' etching method.....	47
2.3.4.3	Rugate reflector etching method.....	48
2.3.5	<i>Pore size gradients</i>	48
2.4	POROUS SILICON MODIFICATION.....	49
2.4.1	<i>Electrochemical modification of porous silicon</i>	49
2.4.1.1	Solutions for electrochemical modification.....	49
Organohalide solutions.....	49	
Alkyne solutions.....	50	
2.4.1.2	Principal uniform electrochemical modification.....	50
Electrochemical organohalide modification method.....	50	
Electrochemical alkyne modification method.....	51	
2.4.1.3	Electrochemical gradient modification.....	52
Electrochemical organohalide gradient modification method.....	52	
2.4.2	<i>Chemical modification of porous silicon using diazonium salts</i>	54
2.4.2.1	Solutions for chemical modification using diazonium salts.....	54
2.4.2.2	Principal uniform chemical modification using diazonium salts.....	54
2.4.2.3	Gradient chemical modification using diazonium salts.....	56
Horizontal diffusion method.....	56	
Vertical diffusion method.....	57	
2.4.3	<i>Deacetylation of pentyl acetate groups attached to porous silicon</i>	58
2.4.4	<i>Deprotonation of undecanoic acid groups attached to porous silicon</i>	59
2.4.5	<i>'Endcapping' surfaces</i>	59
2.4.6	<i>Hydrofluoric acid soak</i>	60
2.5	CHARACTERISATION OF POROUS SILICON SURFACES.....	60
2.5.1	<i>Fourier Transform Infrared Spectroscopy</i>	60
2.5.1.1	Transmission Fourier Transform Infrared Spectroscopy.....	60
2.5.1.2	Attenuated Total Reflectance Fourier Transform Infrared Spectroscopy.....	61
2.5.2	<i>Scanning Electron Microscope</i>	61
2.5.3	<i>UV-visible Reflectance Spectroscopy</i>	61
2.5.4	<i>X-ray photoelectron Spectroscopy</i>	62
2.5.5	<i>Camera</i>	62
2.5.6	<i>Water contact angle measurements</i>	62
2.5.7	<i>Imaging equipment</i>	62
2.5.8	<i>Lighting and other equipment</i>	63
2.5.9	<i>Determination of porosity and thickness of porous silicon</i>	63
2.5.9.1	Gravimetric determination of porosity and thickness.....	63
2.5.9.2	Calculation of porosity from solvent impregnation.....	64
2.6	EXPERIMENTAL DETAILS OF VAPOUR DOSING EXPERIMENTS.....	67
2.6.1	<i>Instrumentation and materials for vapour dosing experiments</i>	67
2.6.1.1	Vapour dosing setup.....	68
2.6.2	<i>Methods for vapour dosing experiments</i>	71
2.6.3	<i>Calibration of solvent vapour concentrations by GC-FID</i>	73
CHAPTER 3 RESULTS OF PREPARATION AND CHARACTERISATION OF MODIFIED		
POROUS SILICON.....		80
3.1	FORMATION OF POROUS SILICON.....	81
3.1.1	<i>Formation of Fabry-Perot porous silicon</i>	81
3.1.2	<i>Formation of 'uniformly etched' n-type silicon</i>	89
3.1.3	<i>Formation of rugate reflector porous silicon</i>	92

3.1.4	<i>Formation of pore size gradients</i>	103
3.1.4.1	Formation of Fabry-Perot pore size gradients.....	103
3.1.4.2	Formation of rugate reflector pore size gradients.....	104
3.2	ELECTROCHEMICAL MODIFICATION OF POROUS SILICON.....	106
3.2.1	<i>Modification using cathodic electrochemical alkyne attachment</i>	106
3.2.1.1	Phenyl acetylene-modified porous silicon.....	107
3.2.1.2	Heptyne-modified porous silicon.....	109
3.2.2	<i>Modification using electrochemical reduction of organohalides</i>	111
3.2.2.1	Methylated porous silicon.....	111
3.2.2.2	Decyl-modified porous silicon.....	119
3.2.2.3	Pentyl acetate-modified porous silicon.....	123
	Pentanol-modified porous silicon.....	127
3.3	GRADIENT FORMATION USING ELECTROCHEMICAL REDUCTION OF ORGANOHALIDES.....	130
3.3.1	<i>Porous silicon modified with a methyl compositional gradient</i>	130
3.3.2	<i>Porous silicon modified with a decyl compositional gradient</i>	135
3.3.3	<i>Porous silicon modified with a pentyl acetate compositional gradient</i>	142
3.3.3.1	Porous silicon modified with a pentanol compositional gradient.....	149
3.3.4	<i>Formation of 2-directional compositional gradients</i>	153
3.4	CHEMICAL HYDROSILYLATION MODIFICATION OF POROUS SILICON USING DIAZONIUM SALTS.....	159
3.4.1	<i>Decyl-modified porous silicon using diazonium salts</i>	160
3.4.2	<i>Undecanoic acid-modified porous silicon using diazonium salts</i>	166
3.4.2.1	Deprotonation of undecanoic acid-modified porous silicon.....	168
3.5	CHEMICAL HYDROSILYLATION GRADIENT MODIFICATION OF POROUS SILICON USING DIAZONIUM SALTS.....	171
3.5.1	<i>Horizontal diffusion of diazonium salts</i>	171
3.5.2	<i>Investigation of uniformity of diffusive processes</i>	171
3.5.3	<i>Vertical diffusion of diazonium salts</i>	173
3.5.3.1	Porous silicon with a decyl compositional gradient using chemical hydrosilylation.....	173
3.5.3.2	Porous silicon with a undecanoic acid compositional gradient using chemical hydrosilylation.....	175
	Porous silicon modified with a deprotonated undecanoic acid compositional gradient.....	178
CHAPTER 4 RESULTS OF VAPOUR DOSING EXPERIMENTS.....		179
4.1	FABRY-PEROT POROUS SILICON MODIFIED USING ELECTROCHEMICAL REDUCTION OF ORGANOHALIDES.....	181
4.1.1	<i>Methylated Fabry-Perot porous silicon</i>	181
4.1.2	<i>Decyl-modified Fabry-Perot porous silicon</i>	189
4.1.3	<i>Pentyl acetate-modified Fabry-Perot porous silicon</i>	197
4.1.4	<i>Pentanol-modified Fabry-Perot porous silicon</i>	204
4.1.5	<i>Summary of vapour dosing of Fabry-Perot porous silicon modified by electrochemical reduction of organohalides</i>	211
4.1.6	<i>Fabry-Perot porous silicon with a gradient of pentyl acetate groups</i>	216
4.1.7	<i>Fabry-Perot porous silicon with a gradient of pentanol groups</i>	221
4.1.8	<i>Summary of compositional gradient modified Fabry-Perot porous silicon modified by electrochemical reduction of organohalides</i>	229
4.2	RUGATE REFLECTOR POROUS SILICON MODIFIED BY CHEMICAL HYDROSILYLATION USING DIAZONIUM SALTS.....	229
4.2.1	<i>Rugate reflector porous silicon modified with a gradient of undecanoic acid groups</i>	229
4.2.2	<i>Rugate reflector porous silicon modified with a gradient of undecanoate groups</i>	240
4.2.3	<i>Summary of compositional gradient modified rugate reflector porous silicon samples modified by chemical hydrosilylation using diazonium salts</i>	246
4.3	IMAGING OF RUGATE REFLECTOR POROUS SILICON SAMPLES.....	246
CHAPTER 5 OVERALL DISCUSSION AND CONCLUSIONS.....		258
5.1	POROUS SILICON SENSORS.....	259
5.1.1	<i>Formation of porous silicon</i>	259
5.1.2	<i>Modification of porous silicon</i>	260
5.1.2.1	Porous silicon surface 'wettability'.....	265

5.1.3	<i>Vapour dosing experiments</i>	268
5.2	CONCLUSIONS.....	276
5.3	FUTURE WORK.....	277
Appendix		280
References		281

List of figures

FIGURE 1-1 DIAGRAM OF AN ELECTROCHEMICAL ETCH CELL.....	6
FIGURE 1-2 MECHANISM OF ATTACHMENT OF ORGANIC GROUPS TO POROUS SILICON VIA ELECTROCHEMICAL REDUCTION OF ORGANOHALIDES.	15
FIGURE 1-3 IR SPECTRUM OF H-TERMINATED POROUS SILICON.	21
FIGURE 1-4 IR SPECTRUM OF A METHYLATED POROUS SILICON SURFACE.	22
FIGURE 1-5 UNCORRECTED REFLECTIVITY SPECTRUM OF A FABRY-PEROT FRINGE POROUS SILICON SAMPLE.	28
FIGURE 1-6 DIAGRAM OF POROUS SILICON AND THE LIGHT INTERACTIONS.	29
FIGURE 1-7 UNCORRECTED REFLECTIVITY SPECTRA OF A RUGATE REFLECTOR POROUS SILICON SAMPLE.....	31
FIGURE 1-8 DIAGRAM SHOWING A SIMPLE MICROFLUIDIC NETWORK (INLETS ARE AT TOP; FLUID FLOWS IN A DOWNWARDS DIRECTION IN DIAGRAM).....	36
FIGURE 2-1 STRUCTURE OF 4-BROMOBENZENEDIAZONIUM TETRAFLUOROBORATE (BBD).....	43
FIGURE 2-2 STRUCTURE OF 3,4,5-TRIFLUOROBENZENEDIAZONIUM TETRAFLUOROBORATE (FBD).	44
FIGURE 2-3 PICTURE OF THE TEFLON ELECTROCHEMICAL CELL WITH ELECTRODES ATTACHED.....	46
FIGURE 2-4 DRAWINGS OF ELECTRODES (A) PLATINUM WIRE, (B) PLATINUM RING AND (C) PLATINUM MESH RING ELECTRODE.	47
FIGURE 2-5 SCHEMATIC DIAGRAM OF THE ASYMMETRIC ELECTROCHEMICAL CELL ANALOGOUS TO THAT USED BY SAILOR. ^{39,40}	49
FIGURE 2-6 PICTURE OF THE GLASS ADAPTER ON THE ELECTROCHEMICAL CELL USED FOR ELECTROCHEMICAL MODIFICATIONS.	51
FIGURE 2-7 SCHEMATIC DIAGRAM OF THE ASYMMETRIC ELECTROCHEMICAL CELL ANALOGOUS TO THAT USED BY SAILOR. ^{39,40}	52
FIGURE 2-8 GRAPH SHOWING CURRENT VERSUS TIME FOR THE FOUR CURRENT DENSITY TECHNIQUES (A) CONSTANT CURRENT, (B) LINEAR CURRENT RAMP, (C) EXPONENTIAL CURRENT RAMP AND (D) CONSTANT CURRENT PLUS LINEAR CURRENT RAMP.	53
FIGURE 2-9 GLASS ADAPTER USED FOR CHEMICAL MODIFICATIONS.....	55
FIGURE 2-10 GLASS ADAPTER WITH SEPTUM FOR GRADIENT CHEMICAL MODIFICATION USING DIAZONIUM SALTS.....	56
FIGURE 2-11 DIAGRAM AND PICTURE OF THE CUSTOM MADE GLASS CONTAINER USED FOR VERTICAL DIFFUSION METHOD.	57
FIGURE 2-12 SCHEMATIC OF VAPOUR DOSING SETUP 1.....	69
FIGURE 2-13 SCHEMATIC OF VAPOUR DOSING SETUP 2.....	71
FIGURE 3-1 SINGLE BEAM TRANSMISSION FTIR BACKGROUND OF A P-TYPE SILICON (RESISTIVITY 1 - 5 Ω CM).	81
FIGURE 3-2 TRANSMISSION FTIR SPECTRUM OF A FABRY-PEROT POROUS SILICON SAMPLE.....	82
FIGURE 3-3 A TYPICAL VISIBLE UNCORRECTED REFLECTIVITY SPECTRUM OF A FABRY-PEROT POROUS SILICON SAMPLE. INSERT SHOWS COLOUR IMAGE OF SUCH A SAMPLE UNDER WHITE LIGHT ILLUMINATION.	83
FIGURE 3-4 SEM IMAGE OF THE TOP SURFACE OF A FABRY-PEROT POROUS SILICON SAMPLE.	84
FIGURE 3-5 SEM IMAGE OF THE CROSS SECTION OF A FABRY-PEROT POROUS SILICON SAMPLE.	85
FIGURE 3-6 DIAGRAM OF THE THICKNESS DIFFERENCES WITH LOW DOPED POROUS SILICON.	85
FIGURE 3-7 UNCORRECTED REFLECTIVITY SPECTRA OF A SINGLE POROUS SILICON SAMPLE IMMERSSED IN DIFFERENT SOLVENTS.	86
FIGURE 3-8 GRAPH OF FRINGE NUMBER (M) VERSUS 1000/WAVELENGTH MAXIMUM FOR FABRY-PEROT POROUS SILICON SAMPLE IMMERSSED IN DIFFERENT SOLVENTS.	87
FIGURE 3-9 GRAPH OF $(EOT/2)^{2/3}$ VERSUS $n^{2/3}$ FOR A SAMPLE OF POROUS SILICON IMMERSSED IN THE SOLVENTS GIVEN IN FIGURE 3-8.	88

FIGURE 3-10 TRANSMISSION FTIR SPECTRUM OF A ‘UNIFORMLY ETCHED’ POROUS SILICON SAMPLE (N-TYPE).	90
FIGURE 3-11 SEM IMAGE OF THE TOP SURFACE OF A ‘UNIFORMLY ETCHED’ POROUS SILICON SAMPLE (N-TYPE).	91
FIGURE 3-12 SEM IMAGE OF THE CROSS SECTION OF A ‘UNIFORMLY ETCHED’ POROUS SILICON SAMPLE (N-TYPE).	92
FIGURE 3-13 TYPICAL ATR FTIR SPECTRUM OF THE KRS5/DIAMOND COMPOSITE CRYSTAL.	93
FIGURE 3-14 ATR FTIR SPECTRUM OF A RUGATE REFLECTOR POROUS SILICON SAMPLE USING A BACKGROUND OF THE KRS5/DIAMOND COMPOSITE CRYSTAL IN AIR.	94
FIGURE 3-15 A VISIBLE UNCORRECTED REFLECTIVITY SPECTRUM OF A RUGATE REFLECTOR POROUS SILICON SAMPLE (CORRESPONDING TO THE LEFT-MOST INSERT). INSERTS SHOW COLOUR IMAGES OF THREE POROUS SILICON RUGATE REFLECTOR SAMPLES ETCHED WITH DIFFERENT PERIODICITIES.	95
FIGURE 3-16 SEM IMAGE OF THE TOP SURFACE OF A RUGATE REFLECTOR POROUS SILICON SAMPLE.	96
FIGURE 3-17 SEM IMAGE OF THE CROSS SECTION OF A RUGATE REFLECTOR POROUS SILICON SAMPLE.	97
FIGURE 3-18 UNCORRECTED REFLECTIVITY SPECTRA OF A SINGLE POROUS SILICON RUGATE IMMERSSED IN DIFFERENT SOLVENTS.	98
FIGURE 3-19 GRAPH OF $\Lambda_{\text{MAX}}^{2/3}$ VERSUS $N^{2/3}$ FOR A POROUS SILICON SAMPLE IMMERSSED IN THE SOLVENTS GIVEN IN FIGURE 3-18.	99
FIGURE 3-20 SCHEMATIC OF AN IMAGE CUBE.	100
FIGURE 3-21 IMAGE OF EIGHT RUGATE REFLECTOR POROUS SILICON SAMPLES (5 – 10 M Ω CM) FROM THE SAME SILICON WAFER IN THEIR INITIAL RELATIVE POSITIONS SHOWING A CIRCULAR PATTERN OF STRIATIONS. IMAGE TAKEN USING LCTF FILTER SET AT 560 NM.	101
FIGURE 3-22 IMAGES OF POROUS SILICON RUGATE REFLECTOR SAMPLES (5 – 10 M Ω CM) WITH PORE SIZE GRADIENTS (A) PERPENDICULAR TO THE STRIATIONS AND (B) PARALLEL TO THE STRIATIONS . IMAGES WERE TAKEN USING AN LCTF FILTER SET AT 620 NM.	102
FIGURE 3-23 IMAGES OF POROUS SILICON RUGATE REFLECTOR SAMPLES USING SILICON WITH A RESISTIVITY OF (A) 5 – 10 M Ω CM AND (B) 0.8 – 1.2 M Ω CM . THESE IMAGES WERE ACQUIRED WITH A LCTF FILTER SET AT 560 AND 526 NM RESPECTIVELY, CORRESPONDING TO A WAVELENGTH CLOSE TO THE RUGATE PEAK FOR EACH SAMPLE	102
FIGURE 3-24 GRAPH OF EOT VS DISTANCE FROM THE EDGE OF THE POROUS SILICON CLOSEST TO THE COUNTER ELECTRODE FOR 3 REPLICATE SAMPLES (----- INDICATED THE POSITION OF THE ASYMMETRIC COUNTER ELECTRODE).	103
FIGURE 3-25 VISIBLE UNCORRECTED REFLECTIVITY SPECTRA OF A RUGATE REFLECTOR POROUS SILICON PORE SIZE GRADIENT. SAMPLE WAS ETCHED WITH A COUNTER ELECTRODE PLACED 2 MM FROM 1 EDGE AND 5 MM ABOVE THE SURFACE. ETCH CONDITIONS: SINUSOIDAL BETWEEN 11.5 AND 34.6 MA CM ⁻² , PERIOD 4.5 S WITH 140 REPEATS.	105
FIGURE 3-26 GRAPH OF RUGATE PEAK POSITION VS DISTANCE FROM EDGE OF THE POROUS SILICON CLOSEST TO THE COUNTER ELECTRODE (----- INDICATED THE POSITION OF THE ASYMMETRIC COUNTER ELECTRODE).	105
FIGURE 3-27 ALKYNE MODIFICATION OF POROUS SILICON WITH PHENYL ACETYLENE OR HEPTYNE.	106
FIGURE 3-28 PROPOSED ANIONIC MECHANISM FOR CATHODIC ELECTROCHEMICAL ALKYNE ATTACHMENT.	107
FIGURE 3-29 TRANSMISSION FTIR SPECTRUM OF A PHENYL ACETYLENE-MODIFIED POROUS SILICON SAMPLE.	108
FIGURE 3-30 TRANSMISSION FTIR SPECTRUM OF A PHENYL ACETYLENE-MODIFIED POROUS SILICON SAMPLE AFTER A HYDROFLUORIC ACID SOAK.	108
FIGURE 3-31 TRANSMISSION FTIR SPECTRUM OF A HEPTYNE-MODIFIED POROUS SILICON SAMPLE.	109
FIGURE 3-32 TRANSMISSION FTIR SPECTRUM OF A HEPTYNE-MODIFIED POROUS SILICON SAMPLE AFTER A HYDROFLUORIC ACID SOAK.	110
FIGURE 3-33 TERMINAL GROUPS THAT HAVE BEEN OBTAINED VIA ELECTROCHEMICAL REDUCTION OF ORGANOHALIDES AT A POROUS SILICON CATHODE (A) DECYL (B) PENTYL ACETATE (C) PENTANOL (D) METHYL.	111
FIGURE 3-34 TRANSMISSION FTIR SPECTRUM OF A METHYLATED FABRY-PEROT POROUS SILICON SAMPLE.	112
FIGURE 3-35 ATR FTIR SPECTRUM OF A METHYLATED FABRY-PEROT POROUS SILICON SAMPLE USING A BACKGROUND OF THE KRS5/DIAMOND COMPOSITE CRYSTAL IN AIR.	113

FIGURE 3-36 TRANSMISSION FTIR SPECTRA OF METHYLATED POROUS SILICON SAMPLES WITH VARYING CATHODIC CURRENT DENSITY FOR 45 S (ETCH TIME 120 S). FOR THE CATHODIC CURRENT DENSITY OF 0 MA CM ⁻² THE POROUS SILICON SAMPLE WAS EXPOSED TO THE ORGANOHALIDE SOLUTION FOR 45 S WITHOUT APPLIED BIAS. (FEATURE AT 2300 CM ⁻¹ IS UNCOMPENSATED ABSORBANCE BY ATMOSPHERIC CO ₂).	114
FIGURE 3-37 TRANSMISSION FTIR SPECTRA AFTER METHYLATION OF POROUS SILICON SAMPLES THAT HAD BEEN PREPARED WITH VARYING ETCH TIMES (FEATURE AT 2300 CM ⁻¹ IS UNCOMPENSATED ABSORBANCE BY ATMOSPHERIC CO ₂). METHYLATION USED A CATHODIC CURRENT DENSITY OF 9 MA CM ⁻² FOR 45 S. ETCHING HAD A CURRENT DENSITY OF 28 MA CM ⁻² .	115
FIGURE 3-38 ATR FTIR SPECTRA AFTER METHYLATION OF POROUS SILICON SAMPLES THAT HAD BEEN PREPARED WITH VARYING ETCH TIMES USING A BACKGROUND OF A DIAMOND CRYSTAL IN AIR. THE BASELINES FOR THESE SPECTRA HAVE BEEN CORRECTED FOR EASE OF GRAPHING (FEATURE AT 2300 CM ⁻¹ IS UNCOMPENSATED ABSORBANCE OF ATMOSPHERIC CO ₂). METHYLATION USED A CATHODIC CURRENT DENSITY OF 9 MA CM ⁻² FOR 45 S. ETCHING HAD A CURRENT DENSITY OF 28 MA CM ⁻² .	116
FIGURE 3-39 TRANSMISSION FTIR SPECTRA OF POROUS SILICON SAMPLES METHYLATED WITH VARYING MODIFICATION TIMES (FEATURE AT 2300 CM ⁻¹ IS UNCOMPENSATED ABSORBANCE OF ATMOSPHERIC CO ₂). METHYLATION USED A CATHODIC CURRENT DENSITY OF 9 MA CM ⁻² . ETCHING HAD A CURRENT DENSITY OF 28 MA CM ⁻² FOR 360 S.	117
FIGURE 3-40 TRANSMISSION FTIR MICROSCOPE MAP SHOWING THE PEAK AREA OF THE SI-CH ₃ ROCKING MODE (AT ~ 770 CM ⁻¹) ACROSS A UNIFORMLY METHYLATED POROUS SILICON SAMPLE (ETCHING HAD A CURRENT DENSITY OF 28 MA CM ⁻² FOR 240 S AND METHYLATION USED A CATHODIC CURRENT DENSITY OF 9 MA CM ⁻² FOR 45 S). THE POROUS SILICON SAMPLE HAS A DIAMETER OF 14 MM.	118
FIGURE 3-41 XPS DEPTH PROFILE OF METHYLATED POROUS SILICON.	119
FIGURE 3-42 TRANSMISSION FTIR SPECTRUM OF DECYL-MODIFIED FABRY-PEROT POROUS SILICON SAMPLE THEN 'ENDCAPPED' WITH METHYL GROUPS.	120
FIGURE 3-43 ATR FTIR SPECTRUM OF A METHYL-ENDCAPPED DECYL-MODIFIED FABRY-PEROT POROUS SILICON SAMPLE USING A BACKGROUND OF THE KRS5/DIAMOND COMPOSITE CRYSTAL IN AIR.	121
FIGURE 3-44 TRANSMISSION FTIR SPECTRA OF POROUS SILICON SAMPLES MODIFIED WITH DECYL GROUPS USING VARYING CATHODIC CURRENT DENSITY WITH A 30 S MODIFICATION TIME. FOR THE CATHODIC CURRENT DENSITY OF 0 MA CM ⁻² THE POROUS SILICON SAMPLE WAS EXPOSED TO THE ORGANOHALIDE SOLUTION FOR 30 S WITHOUT APPLIED BIAS (FEATURE AT 2300 CM ⁻¹ IS UNCOMPENSATED ABSORBANCE BY ATMOSPHERIC CO ₂) POROUS SILICON WAS PREPARED USING AN ETCH TIME OF 120 S AND A CURRENT DENSITY OF 28 MA CM ⁻² .	122
FIGURE 3-45 TRANSMISSION FTIR MICROSCOPE MAP SHOWING CHANGES IN THE PEAK HEIGHT OF THE C-H STRETCHING MODE (AT 2926 CM ⁻¹) ACROSS A DECYL-MODIFIED POROUS SILICON SAMPLE THEN 'ENDCAPPED' WITH METHYL GROUPS.	123
FIGURE 3-46 TRANSMISSION FTIR SPECTRUM OF A PENTYL ACETATE-MODIFIED FABRY-PEROT POROUS SILICON SAMPLE THEN 'ENDCAPPED' WITH METHYL GROUPS.	124
FIGURE 3-47 ATR FTIR SPECTRUM OF A PENTYL ACETATE-MODIFIED FABRY-PEROT POROUS SILICON SAMPLE THEN 'ENDCAPPED' WITH METHYL GROUPS USING A BACKGROUND OF THE KRS5/DIAMOND COMPOSITE CRYSTAL IN AIR.	125
FIGURE 3-48 TRANSMISSION FTIR SPECTRA OF POROUS SILICON SAMPLES MODIFIED WITH PENTYL ACETATE USING VARYING CATHODIC CURRENT DENSITY WITH A MODIFICATION TIME OF 30 S. FOR THE CATHODIC CURRENT DENSITY OF 0 MA CM ⁻² THE POROUS SILICON SAMPLE WAS EXPOSED TO THE ORGANOHALIDE SOLUTION FOR 30 S WITHOUT APPLIED BIAS (FEATURE AT 2300 CM ⁻¹ IS UNCOMPENSATED ABSORBANCE BY ATMOSPHERIC CO ₂). THE POROUS SILICON WAS PREPARED USING AN ETCH TIME OF 28 MA CM ⁻² FOR 120 S.	126
FIGURE 3-49 TRANSMISSION FTIR MICROSCOPE MAP SHOWING CHANGES IN THE PEAK AREA OF THE C-O STRETCHING MODE (AT 1278 CM ⁻¹) ACROSS A PENTYL ACETATE-MODIFIED POROUS SILICON SAMPLE THEN 'ENDCAPPED' WITH METHYL GROUPS.	127
FIGURE 3-50 SCHEMATIC SHOWING THE DEACETYLATION REACTION.	128
FIGURE 3-51 TRANSMISSION FTIR SPECTRA OF (A) PENTYL ACETATE-MODIFIED POROUS SILICON SAMPLE BEFORE DEACETYLATION AND (B) RESULTING PENTANOL-MODIFIED POROUS SILICON SURFACE AFTER DEACETYLATION WITH AMMONIUM CHLORIDE AND CONCENTRATED SULFURIC ACID IN METHANOL (SAMPLES ARE 'ENDCAPPED' WITH METHYL GROUPS).	128

FIGURE 3-52 ATR FTIR SPECTRUM OF A PENTANOL-MODIFIED FABRY-PEROT POROUS SILICON SAMPLE THEN 'ENDCAPPED' WITH METHYL GROUPS USING A BACKGROUND OF THE KRS5/DIAMOND COMPOSITE CRYSTAL IN AIR.	129
FIGURE 3-53 ATR FTIR SPECTRA OF A FABRY-PEROT POROUS SILICON SAMPLE METHYLATED USING AN ASYMMETRIC ELECTRODE PLACEMENT AND A CONSTANT CURRENT (CATHODIC CURRENT DENSITY OF 5 MA CM ⁻² FOR 30 S). SPECTRA ARE MEASURED AT DIFFERENT POSITIONS ACROSS THE SURFACE MOVING AWAY FROM THE EDGE OF THE POROUS SILICON CLOSEST TO THE ASYMMETRIC ELECTRODE (THE REGIONS CORRESPONDING TO THE WATER BAND BETWEEN 1900 AND 1400 CM ⁻¹ AND THE CARBON DIOXIDE BAND BETWEEN 2450 AND 2280 CM ⁻¹ HAVE BEEN ADJUSTED TO ZERO. THE FEATURE AT 650 CM ⁻¹ IS AN INSTRUMENT ARTIFACT). A BACKGROUND OF A DIAMOND CRYSTAL IN AIR WAS USED. THE BASELINES FOR THESE SPECTRA HAVE BEEN CORRECTED TO ALLOW STACKING OF THE SPECTRA.	131
FIGURE 3-54 ATR FTIR SPECTRA OF A FABRY-PEROT POROUS SILICON SAMPLE METHYLATED USING AN ASYMMETRIC ELECTRODE PLACEMENT AND A LINEAR CURRENT RAMP (CATHODIC CURRENT OF 1-8 MA CM ⁻² FOR 60 S) MEASURED AT DIFFERENT POSITIONS ACROSS THE SURFACE MOVING AWAY FROM THE EDGE OF THE POROUS SILICON CLOSEST TO THE ASYMMETRIC ELECTRODE. A BACKGROUND OF A DIAMOND CRYSTAL IN AIR WAS USED. THE BASELINES FOR THESE SPECTRA HAVE BEEN CORRECTED FOR EASE OF GRAPHING.	132
FIGURE 3-55 ATR FTIR SPECTRA OF A FABRY-PEROT POROUS SILICON SAMPLE METHYLATED USING AN ASYMMETRIC ELECTRODE PLACEMENT AND A EXPONENTIAL CURRENT RAMP (CATHODIC CURRENT OF 1-8 MA CM ⁻² FOR 60 S) MEASURED AT DIFFERENT POSITIONS ACROSS THE SURFACE MOVING AWAY FROM THE EDGE OF THE POROUS SILICON CLOSEST TO THE ASYMMETRIC ELECTRODE. A BACKGROUND OF A DIAMOND CRYSTAL IN AIR WAS USED. THE BASELINES FOR THESE SPECTRA HAVE BEEN CORRECTED FOR EASE OF GRAPHING.	133
FIGURE 3-56 ATR FTIR SPECTRA OF A METHYLATED FABRY-PEROT POROUS SILICON SAMPLE USING AN ASYMMETRIC ELECTRODE PLACEMENT AND A CONSTANT THEN LINEAR CURRENT RAMP (CATHODIC CURRENT DENSITY OF 4-8 MA CM ⁻² FOR 60 S) MEASURED AT DIFFERENT POSITIONS ACROSS THE SURFACE MOVING AWAY FROM THE EDGE OF THE POROUS SILICON CLOSEST TO THE ELECTRODE. A BACKGROUND OF A DIAMOND CRYSTAL IN AIR WAS USED. THE BASELINES FOR THESE SPECTRA HAVE BEEN CORRECTED FOR EASE OF GRAPHING.	134
FIGURE 3-57 ATR FTIR SPECTRA OF A DECYL-MODIFIED FABRY-PEROT POROUS SILICON SAMPLE USING AN ASYMMETRIC ELECTRODE PLACEMENT AND A CONSTANT CATHODIC CURRENT (5 MA CM ⁻² FOR 30 S) MEASURED AT DIFFERENT POSITIONS ACROSS THE SURFACE MOVING AWAY FROM THE EDGE OF THE POROUS SILICON CLOSEST TO THE ASYMMETRIC ELECTRODE. A BACKGROUND OF A DIAMOND CRYSTAL IN AIR WAS USED. THE BASELINES FOR THESE SPECTRA HAVE BEEN CORRECTED FOR EASE OF GRAPHING.	136
FIGURE 3-58 ATR FTIR SPECTRA OF A DECYL-MODIFIED FABRY-PEROT POROUS SILICON SAMPLE USING AN ASYMMETRIC ELECTRODE PLACEMENT AND A LINEAR CURRENT DENSITY RAMP (CATHODIC CURRENT DENSITY OF 1-5 MA CM ⁻² FOR 45 S) MEASURED AT DIFFERENT POSITIONS ACROSS THE SURFACE MOVING AWAY FROM THE EDGE OF THE POROUS SILICON CLOSEST TO THE ASYMMETRIC ELECTRODE. A BACKGROUND OF A DIAMOND CRYSTAL IN AIR WAS USED. THE BASELINES FOR THESE SPECTRA HAVE BEEN CORRECTED FOR EASE OF GRAPHING.	137
FIGURE 3-59 TRANSMISSION FTIR MICROSCOPE MAP SHOWING CHANGES IN THE PEAK HEIGHT OF THE C-H STRETCHING MODE (AT 2926 CM ⁻¹) ACROSS A POROUS SILICON SAMPLE WITH A GRADIENT OF DECYL GROUPS THEN 'ENDCAPPED' WITH METHYL GROUPS (○ASYMMETRIC ELECTRODE POSITION, CATHODIC CURRENT DENSITY OF 1 TO 5 MA CM ⁻² FOR 45 S). THE INSERT SHOWS AN ENLARGEMENT OF THE C-H STRETCHING MODE; THE BAND IN THE MIDDLE WAS MONITORED FOR THE MICROSCOPE MAP. TRANSMISSION FTIR LINE MAP (SHOWN BELOW THE AREA MAP) EXTRACTED FROM AREA MAP SHOWING THE HEIGHT OF THE C-H STRETCHING MODE (AT 2926 CM ⁻¹) ACROSS THE POROUS SILICON SAMPLE (_____ INDICATES THE POSITION OF THE ASYMMETRIC ELECTRODE).	138
FIGURE 3-60 TRANSMISSION FTIR MICROSCOPE MAP SHOWING CHANGES IN THE PEAK AREA OF THE Si-CH ₃ ROCKING MODE (AT 770 CM ⁻¹) ACROSS A POROUS SILICON SAMPLE WITH A GRADIENT OF DECYL GROUPS AND 'ENDCAPPED' WITH METHYL GROUPS. TRANSMISSION FTIR LINE MAP (SHOWN BELOW THE AREA MAP) SHOWING THE AREA OF THE Si-CH ₃ ROCKING MODE (AT 770 CM ⁻¹) ACROSS THE POROUS SILICON SAMPLE.	139

FIGURE 3-61 TRANSMISSION FTIR SPECTRA EXTRACTED FROM THE POSITIONS INDICATED IN THE COLOUR IMAGE OF A POROUS SILICON SAMPLE WITH A GRADIENT OF DECYL GROUPS THEN ‘ENDCAPPED’ WITH METHYL GROUPS (○ASYMMETRIC ELECTRODE POSITION).....	141
FIGURE 3-62 ATR FTIR SPECTRA OF A PENTYL ACETATE-MODIFIED FABRY-PEROT POROUS SILICON SAMPLE USING AN ASYMMETRIC ELECTRODE PLACEMENT AND A CONSTANT CATHODIC CURRENT (5 MA CM ⁻² FOR 30 S) MEASURED AT DIFFERENT POSITIONS ACROSS THE SURFACE MOVING AWAY FROM THE EDGE OF THE POROUS SILICON CLOSEST TO THE ASYMMETRIC ELECTRODE. A BACKGROUND OF A DIAMOND CRYSTAL IN AIR WAS USED. THE BASELINES FOR THESE SPECTRA HAVE BEEN CORRECTED FOR EASE OF GRAPHING.	143
FIGURE 3-63 ATR FTIR SPECTRA OF A PENTYL ACETATE-MODIFIED FABRY-PEROT POROUS SILICON SAMPLE USING AN ASYMMETRIC ELECTRODE PLACEMENT AND A LINEAR CURRENT RAMP (CATHODIC CURRENT DENSITY OF 1-5 MA CM ⁻² FOR 45 S) MEASURED AT DIFFERENT POSITIONS ACROSS THE SURFACE MOVING AWAY FROM THE EDGE OF THE POROUS SILICON CLOSEST TO THE ASYMMETRIC ELECTRODE. A BACKGROUND OF A DIAMOND CRYSTAL IN AIR WAS USED. THE BASELINES FOR THESE SPECTRA HAVE BEEN CORRECTED FOR EASE OF GRAPHING.....	144
FIGURE 3-64 TRANSMISSION FTIR MICROSCOPE MAP SHOWING CHANGES IN THE PEAK AREA OF THE C-O STRETCHING MODE (AT 1240 CM ⁻¹) ACROSS A POROUS SILICON SAMPLE WITH A GRADIENT OF PENTYL ACETATE GROUPS THEN ‘ENDCAPPED’ WITH METHYL GROUPS (○ASYMMETRIC ELECTRODE POSITION, CATHODIC CURRENT DENSITY OF 1 TO 5 MA CM ⁻² FOR 45 S). TRANSMISSION FTIR LINE MAP (SHOWN BELOW THE AREA MAP) EXTRACTED FROM AREA MAP SHOWING THE AREA OF THE C-O STRETCHING MODE (AT 1240 CM ⁻¹) AND A LINE MAP OF THE C=O STRETCHING MODE (AT 1750 CM ⁻¹) ACROSS THE POROUS SILICON SAMPLE IS SHOWN UNDER THE C-O LINE MAP (----- INDICATES THE POSITION OF THE ASYMMETRIC ELECTRODE).	146
FIGURE 3-65 TRANSMISSION FTIR SPECTRA EXTRACTED FROM THE POSITIONS INDICATED IN THE COLOUR IMAGE OF A POROUS SILICON SAMPLE WITH A GRADIENT OF PENTYL ACETATE GROUPS THEN ‘ENDCAPPED’ WITH METHYL GROUPS (○ASYMMETRIC ELECTRODE POSITION).	148
FIGURE 3-66 TRANSMISSION FTIR MICROSCOPE MAP SHOWING CHANGES IN THE PEAK AREA OF THE C-O STRETCHING MODE (AT 1240 CM ⁻¹) ACROSS A POROUS SILICON SAMPLE WITH A GRADIENT OF PENTYL ACETATE GROUPS THEN ‘ENDCAPPED’ WITH METHYL GROUPS BEFORE DEACETYLATION TO FORM PENTANOL GROUPS (○ASYMMETRIC ELECTRODE POSITION, CATHODIC CURRENT DENSITY OF 1 TO 5 MA CM ⁻² FOR 45 S) . TRANSMISSION FTIR LINE MAP (SHOWN BELOW THE AREA MAP) EXTRACTED FROM AREA MAP SHOWING THE AREA OF THE C-O STRETCHING MODE (AT 1240 CM ⁻¹) ACROSS THE POROUS SILICON SAMPLE (----- INDICATES THE POSITION OF THE ASYMMETRIC ELECTRODE).	150
FIGURE 3-67 TRANSMISSION FTIR SPECTRA EXTRACTED FROM THE POSITIONS INDICATED IN THE COLOUR IMAGE OF A POROUS SILICON SAMPLE WITH A GRADIENT OF PENTYL ACETATE GROUPS THEN ‘ENDCAPPED’ WITH METHYL GROUPS BEFORE DEACETYLATION (○ASYMMETRIC ELECTRODE POSITION).....	152
FIGURE 3-68 TRANSMISSION FTIR MICROSCOPE MAP SHOWING CHANGES IN THE PEAK HEIGHT OF THE C-H STRETCHING MODE (AT 2926 CM ⁻¹) AND THE PEAK AREA OF THE SI-CH ₃ ROCKING MODE (AT 770 CM ⁻¹) ACROSS A POROUS SILICON SAMPLE WITH A GRADIENT OF DECYL AND METHYL GROUPS IN OPPOSITE DIRECTIONS (○ASYMMETRIC ELECTRODE POSITION, DECYL; CATHODIC CURRENT DENSITY 1 TO 5 MA CM ⁻² FOR 45 S. METHYL; CATHODIC CURRENT DENSITY OF 1 TO 8 MA CM ⁻² FOR 60 S)	154
FIGURE 3-69 TRANSMISSION FTIR SPECTRA EXTRACTED FROM THE POSITIONS INDICATED IN THE COLOUR IMAGE OF A POROUS SILICON SAMPLE WITH A GRADIENT OF DECYL AND METHYL GROUPS IN OPPOSITE DIRECTIONS (■ASYMMETRIC ELECTRODE POSITION FOR DECYL MODIFICATION AND ■ASYMMETRIC ELECTRODE POSITION FOR METHYL MODIFICATION).	155
FIGURE 3-70 TRANSMISSION FTIR MICROSCOPE MAP SHOWING CHANGES IN THE PEAK AREA OF THE C-O STRETCHING MODE (AT 1240 CM ⁻¹) AND THE SI-CH ₃ ROCKING MODE (AT 770 CM ⁻¹) ACROSS A POROUS SILICON SAMPLE WITH A GRADIENT OF PENTYL ACETATE AND METHYL GROUPS IN OPPOSITE DIRECTIONS (○ASYMMETRIC ELECTRODE POSITION, PENTYL ACETATE; CATHODIC CURRENT DENSITY OF 1 TO 5 MA CM ⁻² FOR 45 S. METHYL; CATHODIC CURRENT DENSITY OF 1 TO 8 MA CM ⁻² FOR 60 S). THE INSERT OF A COLOUR IMAGE, FIGURE 3-71 OF THE POROUS SILICON SAMPLE SHOWS A SCRATCH ON THE RIGHT SIDE OF THE SAMPLE WHICH HAS AFFECTED THE TRANSMISSION FTIR MAPS.	157
FIGURE 3-71 TRANSMISSION FTIR SPECTRA EXTRACTED FROM THE POSITIONS INDICATED IN THE COLOUR IMAGE OF A POROUS SILICON SAMPLE WITH A GRADIENT OF PENTYL ACETATE AND METHYL GROUPS IN	






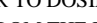
OPPOSITE DIRECTIONS (ASYMMETRIC ELECTRODE POSITION FOR PENTYL ACETATE MODIFICATION AND OPPOSITE FOR THE PLACEMENT OF THE ASYMMETRIC ELECTRODE POSITION FOR METHYL MODIFICATION). THE INSERT COLOUR IMAGE SHOWS A LARGE SCRATCH ON THE RIGHT SIDE WHICH HAS AFFECTED THE TRANSMISSION FTIR MAPPING DATA IN FIGURE 3-70.	158
FIGURE 3-72 TERMINAL GROUPS THAT HAVE BEEN GRAFTED ONTO POROUS SILICON BY CHEMICAL HYDROSILYLATION (A) DECYL (B) UNDECANOIC ACID.	159
FIGURE 3-73 PROPOSED MECHANISM FOR CHEMICAL HYDROSILYLATION USING DIAZONIUM SALTS.	160
FIGURE 3-74 TRANSMISSION FTIR SPECTRA OF FABRY-PEROT POROUS SILICON SAMPLES MODIFIED USING (A) FBD OR (B) BBD DIAZONIUM SALTS AND NEAT DECENE.	161
FIGURE 3-75 TRANSMISSION FTIR SPECTRA OF A DECYL MODIFIED FABRY-PEROT POROUS SILICON SAMPLE (A) AFTER MODIFICATION WITH NEAT DECENE (B) AFTER A HYDROFLUORIC ACID SOAK.	162
FIGURE 3-76 TRANSMISSION FTIR SPECTRUM OF A DECYL-MODIFIED FABRY-PEROT POROUS SILICON SAMPLE (MODIFIED USING FBD-INITIATED HYDROSILYLATION AND 'ENDCAPPED' USING ELECTROCHEMICAL METHODS).	163
FIGURE 3-77 ATR FTIR SPECTRUM OF A DECYL-MODIFIED RUGATE REFLECTOR POROUS SILICON SAMPLE USING A BACKGROUND OF THE KRS5/DIAMOND COMPOSITE CRYSTAL IN AIR (MODIFIED USING FBD-INITIATED HYDROSILYLATION AND 'ENDCAPPED' USING ELECTROCHEMICAL METHODS).	163
FIGURE 3-78 TRANSMISSION FTIR MICROSCOPE MAP SHOWING THE PEAK HEIGHT OF THE C-H STRETCHING MODE (AT 2926 cm^{-1}) ACROSS A FABRY-PEROT POROUS SILICON SAMPLE WITH DECYL GROUPS THEN 'ENDCAPPED' WITH METHYL GROUPS (FBD, 3 H). THE SMALL FEATURES IN THE BOTTOM RIGHT CORNER CORRELATE WITH SCRATCH MARKS OBSERVED ON THE POROUS SILICON SURFACE.	164
FIGURE 3-79 TRANSMISSION FTIR SPECTRA OF A FABRY-PEROT POROUS SILICON SAMPLE MODIFIED WITH (A) DECENE (B) UNDECANOIC ACID IN TETRAHYDROFURAN (FBD, 3 H).	166
FIGURE 3-80 TRANSMISSION FTIR SPECTRUM OF AN UNDECANOIC ACID-MODIFIED FABRY PEROT POROUS SILICON SAMPLE (MODIFIED USING FBD-INITIATED HYDROSILYLATION AND 'ENDCAPPED' USING ELECTROCHEMICAL METHODS).	166
FIGURE 3-81 ATR FTIR SPECTRUM OF AN UNDECANOIC ACID-MODIFIED RUGATE REFLECTOR POROUS SILICON SAMPLE USING A BACKGROUND OF THE KRS5/DIAMOND COMPOSITE CRYSTAL IN AIR (MODIFIED USING FBD-INITIATED HYDROSILYLATION AND 'ENDCAPPED' USING ELECTROCHEMICAL METHODS).	167
FIGURE 3-82 TRANSMISSION FTIR MICROSCOPE MAP SHOWING CHANGES IN THE PEAK HEIGHT OF THE C-H STRETCHING MODE (AT 2929 cm^{-1}) ACROSS A FABRY-PEROT POROUS SILICON SAMPLE WITH UNDECANOIC ACID GROUPS THEN 'ENDCAPPED' WITH METHYL GROUPS (FBD, 3 H). THE TOP LEFT CORNER SHOWS SCRATCH MARKS.	168
FIGURE 3-83 SCHEMATIC SHOWING THE DEPROTONATION REACTION.	169
FIGURE 3-84 ATR FTIR SPECTRA OF (A) UNDECANOIC ACID-MODIFIED POROUS SILICON SAMPLE PROTONATED AND (B) UNDECANOIC ACID-MODIFIED POROUS SILICON SURFACE AFTER DEPROTONATION WITH POTASSIUM HYDROXIDE (SAMPLES ARE 'ENDCAPPED' WITH METHYL GROUPS).	170
FIGURE 3-85 HORIZONTAL DIFFUSION SHOWING CONTAINER EDGE EFFECTS (A GLASS CONTAINER WITH A 5 CM DIAMETER AND A HEIGHT OF 3 CM, A GLASS FRIT WITH A DIAMETER OF 20 MM WAS PLACED IN THE CONTAINER, 3 mL OF 2:1 THF:ACETONITRILE WAS USED AS THE BULK SOLVENT AND 20 μL OF CRYSTAL VIOLET IN ACETONITRILE WERE ADDED ON TOP OF THE GLASS FRIT, THE DEPTH OF SOLUTION IS APPROXIMATELY 5 MM).	171
FIGURE 3-86 HORIZONTAL DIFFUSION EXPERIMENTS WITH THE DYE CRYSTAL VIOLET SHOWING CONVECTION EFFECTS AND GENERAL NON-UNIFORM MOVEMENT (A GLASS PETRI DISH WITH A DIAMETER OF 10 CM WAS USED FOR THE THREE IMAGES IN THE TOP ROW AND A DISH WITH A DIAMETER OF 15 CM WAS USED FOR THE TWO IMAGES IN THE BOTTOM ROW).	172
FIGURE 3-87 VERTICAL DIFFUSION WITHOUT AND WITH A SILICON WAFER PRESENT IN THE MAIN CHAMBER (DIMENSIONS OF THE CUSTOM MADE GLASS CONTAINER ARE: MAIN CHAMBER IS 2.5 x 2.5 x 0.5 CM AND THE DIAMETER OF THE SIDE ARM IS 2.5 MM, 1 mL OF 2:1 THF:ACETONITRILE WAS USED AS THE BULK SOLVENT AND 10 μL OF CRYSTAL VIOLET IN 2:1 THF:ACETONITRILE WERE ADDED INTO THE SIDE ARM, PHOTOGRAPHS WERE CAPTURED 9 H 40 MIN AND 13 H AFTER DYE WAS ADDED INTO THE SIDE ARM).	172
FIGURE 3-88 ATR FTIR SPECTRA OF A DECYL-MODIFIED RUGATE REFLECTOR POROUS SILICON SAMPLE (FBD, 3 H 45 MIN) MEASURED AT DIFFERENT POSITIONS ACROSS THE SAMPLE PARALLEL WITH THE GRADIENT DIRECTION USING A BACKGROUND OF THE KRS5/DIAMOND COMPOSITE CRYSTAL IN AIR.	174

FIGURE 3-89 ATR FTIR SPECTRA OF A DECYL-MODIFIED RUGATE REFLECTOR POROUS SILICON SAMPLE MEASURED PERPENDICULAR TO THE GRADIENT DIRECTION USING A BACKGROUND OF THE KRS5/DIAMOND COMPOSITE CRYSTAL IN AIR.....	174
FIGURE 3-90 ATR FTIR SPECTRA OF AN UNDECANOIC ACID-MODIFIED RUGATE REFLECTOR POROUS SILICON SAMPLE (FBD, 3 H 15 MIN) MEASURED AT DIFFERENT POSITIONS ACROSS THE SAMPLE PARALLEL WITH THE GRADIENT DIRECTION USING A BACKGROUND OF THE KRS5/DIAMOND COMPOSITE CRYSTAL IN AIR.....	176
FIGURE 3-91 ATR FTIR SPECTRA OF AN UNDECANOIC ACID-MODIFIED RUGATE REFLECTOR POROUS SILICON SAMPLE MEASURED PERPENDICULAR TO THE GRADIENT DIRECTION USING A BACKGROUND OF THE KRS5/DIAMOND COMPOSITE CRYSTAL IN AIR.....	176
FIGURE 3-92 DUPLICATE IMAGES OF WATER DROPLETS PLACED ALONG THE DIRECTION OF THE UNDECANOIC ACID COMPOSITIONAL GRADIENT ( SHOWS THE DIRECTION OF THE GRADIENT FROM HIGHEST TO LOWEST CONCENTRATION OF UNDECANOIC ACID GROUPS).....	177
FIGURE 3-93 DUPLICATE IMAGES OF WATER DROPLETS PLACED ALONG THE DIRECTION OF THE UNDECANOATE COMPOSITIONAL GRADIENT ( SHOWS THE DIRECTION OF THE GRADIENT FROM HIGHEST TO LOWEST CONCENTRATION OF UNDECANOATE GROUPS).....	178
FIGURE 4-1 STRUCTURE OF THE SOLVENTS USED FOR VAPOUR DOSING EXPERIMENTS.....	180
FIGURE 4-2 THE OPTICAL RESPONSE OF A METHYLATED FABRY-PEROT POROUS SILICON SAMPLE DOSED WITH ETHANOL VAPOUR. THE TOP GRAPH PLOTS THE EOT VS TIME FOR SPATIAL POSITION 3 (LABELS ON TOP OF EACH PULSE SHOW THE P/P _s VALUE FOR EACH PULSE). THE BOTTOM GRAPH PLOTS THE RESPONSE NORMALIZED TO THE VALUE OBTAINED AT THE HIGHEST CONCENTRATION VS P/P _s (CLOSED SYMBOLS ARE INCREASING PULSES AND OPEN SYMBOLS ARE DECREASING PULSES). RESPONSE = $\Delta EOT / \Delta EOT_{MAX}$	185
FIGURE 4-3 THE OPTICAL RESPONSE OF A METHYLATED FABRY-PEROT POROUS SILICON SAMPLE DOSED WITH HEPTANE VAPOUR. THE TOP GRAPH PLOTS THE EOT VS TIME FOR SPATIAL POSITION 1 (LABELS ON TOP OF EACH PULSE SHOW THE P/P _s VALUE FOR EACH PULSE). THE BOTTOM GRAPH PLOTS THE RESPONSE NORMALIZED TO THE VALUE OBTAINED AT THE HIGHEST CONCENTRATION VS P/P _s (CLOSED SYMBOLS ARE INCREASING PULSES AND OPEN SYMBOLS ARE DECREASING PULSES). RESPONSE = $\Delta EOT / \Delta EOT_{MAX}$	186
FIGURE 4-4 THE OPTICAL RESPONSE OF A METHYLATED FABRY-PEROT POROUS SILICON SAMPLE DOSED WITH TOLUENE VAPOUR. THE TOP GRAPH PLOTS THE EOT VS TIME FOR SPATIAL POSITION 2 (LABELS ON TOP OF EACH PULSE SHOW THE P/P _s VALUE FOR EACH PULSE). THE BOTTOM GRAPH PLOTS THE RESPONSE NORMALIZED TO THE VALUE OBTAINED AT THE HIGHEST CONCENTRATION VS P/P _s (CLOSED SYMBOLS ARE INCREASING PULSES AND OPEN SYMBOLS ARE DECREASING PULSES). RESPONSE = $\Delta EOT / \Delta EOT_{MAX}$	187
FIGURE 4-5 THE OPTICAL RESPONSE OF A METHYLATED FABRY-PEROT POROUS SILICON SAMPLE DOSED WITH 2-HEXANOL VAPOUR. THE TOP GRAPH PLOTS THE EOT VS TIME FOR SPATIAL POSITION 2 (LABELS ON TOP OF EACH PULSE SHOW THE P/P _s VALUE FOR EACH PULSE). THE BOTTOM GRAPH PLOTS THE RESPONSE NORMALIZED TO THE VALUE OBTAINED AT THE HIGHEST CONCENTRATION VS P/P _s (CLOSED SYMBOLS ARE INCREASING PULSES AND OPEN SYMBOLS ARE DECREASING PULSES). RESPONSE = $\Delta EOT / \Delta EOT_{MAX}$	188
FIGURE 4-6 THE OPTICAL RESPONSE OF A DECYL-MODIFIED FABRY-PEROT POROUS SILICON SAMPLE DOSED WITH ETHANOL VAPOUR. THE TOP GRAPH PLOTS THE EOT VS TIME FOR SPATIAL POSITION 2 (LABELS ON TOP OF EACH PULSE SHOW THE P/P _s VALUE FOR EACH PULSE). THE BOTTOM GRAPH PLOTS THE RESPONSE NORMALIZED TO THE VALUE OBTAINED AT THE HIGHEST CONCENTRATION VS P/P _s (CLOSED SYMBOLS ARE INCREASING PULSES AND OPEN SYMBOLS ARE DECREASING PULSES). RESPONSE = $\Delta EOT / \Delta EOT_{MAX}$	193
FIGURE 4-7 THE OPTICAL RESPONSE OF A DECYL-MODIFIED FABRY-PEROT POROUS SILICON SAMPLE DOSED WITH HEPTANE VAPOUR. THE TOP GRAPH PLOTS THE EOT VS TIME FOR SPATIAL POSITION 2 (LABELS ON TOP OF EACH PULSE SHOW THE P/P _s VALUE FOR EACH PULSE). THE BOTTOM GRAPH PLOTS THE RESPONSE NORMALIZED TO THE VALUE OBTAINED AT THE HIGHEST CONCENTRATION VS P/P _s (CLOSED SYMBOLS ARE INCREASING PULSES AND OPEN SYMBOLS ARE DECREASING PULSES). RESPONSE = $\Delta EOT / \Delta EOT_{MAX}$	194
FIGURE 4-8 THE OPTICAL RESPONSE OF A DECYL-MODIFIED FABRY-PEROT POROUS SILICON SAMPLE DOSED WITH TOLUENE VAPOUR. THE TOP GRAPH PLOTS THE EOT VS TIME FOR SPATIAL POSITION 2 (LABELS ON TOP OF EACH PULSE SHOW THE P/P _s VALUE FOR EACH PULSE). THE BOTTOM GRAPH PLOTS THE	

RESPONSE NORMALIZED TO THE VALUE OBTAINED AT THE HIGHEST CONCENTRATION VS P/P_s (CLOSED SYMBOLS ARE INCREASING PULSES AND OPEN SYMBOLS ARE DECREASING PULSES). RESPONSE = $\Delta EOT / \Delta EOT_{MAX}$	195
FIGURE 4-9 THE OPTICAL RESPONSE OF A DECYL-MODIFIED FABRY-PEROT POROUS SILICON SAMPLE DOSED WITH 2-HEXANOL VAPOUR. THE TOP GRAPH PLOTS THE EOT VS TIME FOR SPATIAL POSITION 2 (LABELS ON TOP OF EACH PULSE SHOW THE P/P_s VALUE FOR EACH PULSE). THE BOTTOM GRAPH PLOTS THE RESPONSE NORMALIZED TO THE VALUE OBTAINED AT THE HIGHEST CONCENTRATION VS P/P_s (CLOSED SYMBOLS ARE INCREASING PULSES AND OPEN SYMBOLS ARE DECREASING PULSES). RESPONSE = $\Delta EOT / \Delta EOT_{MAX}$	196
FIGURE 4-10 THE OPTICAL RESPONSE OF A PENTYL ACETATE-MODIFIED FABRY-PEROT POROUS SILICON SAMPLE DOSED WITH ETHANOL VAPOUR. THE TOP GRAPH PLOTS THE EOT VS TIME FOR SPATIAL POSITION 2 (LABELS ON TOP OF EACH PULSE SHOW THE P/P_s VALUE FOR EACH PULSE). THE BOTTOM GRAPH PLOTS THE RESPONSE NORMALIZED TO THE VALUE OBTAINED AT THE HIGHEST CONCENTRATION VS P/P_s (CLOSED SYMBOLS ARE INCREASING PULSES AND OPEN SYMBOLS ARE DECREASING PULSES). RESPONSE = $\Delta EOT / \Delta EOT_{MAX}$	200
FIGURE 4-11 THE OPTICAL RESPONSE OF A PENTYL ACETATE-MODIFIED FABRY-PEROT POROUS SILICON SAMPLE DOSED WITH HEPTANE VAPOUR. THE TOP GRAPH PLOTS THE EOT VS TIME FOR SPATIAL POSITION 1 (LABELS ON TOP OF EACH PULSE SHOW THE P/P_s VALUE FOR EACH PULSE). THE BOTTOM GRAPH PLOTS THE RESPONSE NORMALIZED TO THE VALUE OBTAINED AT THE HIGHEST CONCENTRATION VS P/P_s (CLOSED SYMBOLS ARE INCREASING PULSES AND OPEN SYMBOLS ARE DECREASING PULSES). RESPONSE = $\Delta EOT / \Delta EOT_{MAX}$	201
FIGURE 4-12 THE OPTICAL RESPONSE OF A PENTYL ACETATE-MODIFIED FABRY-PEROT POROUS SILICON SAMPLE DOSED WITH TOLUENE VAPOUR. THE TOP GRAPH PLOTS THE EOT VS TIME FOR SPATIAL POSITION 2 (LABELS ON TOP OF EACH PULSE SHOW THE P/P_s VALUE FOR EACH PULSE). THE BOTTOM GRAPH PLOTS THE RESPONSE NORMALIZED TO THE VALUE OBTAINED AT THE HIGHEST CONCENTRATION VS P/P_s (CLOSED SYMBOLS ARE INCREASING PULSES AND OPEN SYMBOLS ARE DECREASING PULSES). RESPONSE = $\Delta EOT / \Delta EOT_{MAX}$	202
FIGURE 4-13 THE OPTICAL RESPONSE OF A PENTYL ACETATE-MODIFIED FABRY-PEROT POROUS SILICON SAMPLE DOSED WITH 2-HEXANOL VAPOUR. THE TOP GRAPH PLOTS THE EOT VS TIME FOR SPATIAL POSITION 2 (LABELS ON TOP OF EACH PULSE SHOW THE P/P_s VALUE FOR EACH PULSE). THE BOTTOM GRAPH PLOTS THE RESPONSE NORMALIZED TO THE VALUE OBTAINED AT THE HIGHEST CONCENTRATION VS P/P_s (CLOSED SYMBOLS ARE INCREASING PULSES AND OPEN SYMBOLS ARE DECREASING PULSES). RESPONSE = $\Delta EOT / \Delta EOT_{MAX}$	203
FIGURE 4-14 THE OPTICAL RESPONSE OF A PENTANOL-MODIFIED FABRY-PEROT POROUS SILICON SAMPLE DOSED WITH ETHANOL VAPOUR. THE TOP GRAPH PLOTS THE EOT VS TIME FOR SPATIAL POSITION 2 (LABELS ON TOP OF EACH PULSE SHOW THE P/P_s VALUE FOR EACH PULSE). THE BOTTOM GRAPH PLOTS THE RESPONSE NORMALIZED TO THE VALUE OBTAINED AT THE HIGHEST CONCENTRATION VS P/P_s (CLOSED SYMBOLS ARE INCREASING PULSES AND OPEN SYMBOLS ARE DECREASING PULSES). RESPONSE = $\Delta EOT / \Delta EOT_{MAX}$	207
FIGURE 4-15 THE OPTICAL RESPONSE OF A PENTANOL-MODIFIED FABRY-PEROT POROUS SILICON SAMPLE DOSED WITH HEPTANE VAPOUR. THE TOP GRAPH PLOTS THE EOT VS TIME FOR SPATIAL POSITION 2 (LABELS ON TOP OF EACH PULSE SHOW THE P/P_s VALUE FOR EACH PULSE). THE BOTTOM GRAPH PLOTS THE RESPONSE NORMALIZED TO THE VALUE OBTAINED AT THE HIGHEST CONCENTRATION VS P/P_s (CLOSED SYMBOLS ARE INCREASING PULSES AND OPEN SYMBOLS ARE DECREASING PULSES). RESPONSE = $\Delta EOT / \Delta EOT_{MAX}$	208
FIGURE 4-16 THE OPTICAL RESPONSE OF A PENTANOL-MODIFIED FABRY-PEROT POROUS SILICON SAMPLE DOSED WITH TOLUENE VAPOUR. THE TOP GRAPH PLOTS THE EOT VS TIME FOR SPATIAL POSITION 2 (LABELS ON TOP OF EACH PULSE SHOW THE P/P_s VALUE FOR EACH PULSE). THE BOTTOM GRAPH PLOTS THE RESPONSE NORMALIZED TO THE VALUE OBTAINED AT THE HIGHEST CONCENTRATION VS P/P_s (CLOSED SYMBOLS ARE INCREASING PULSES AND OPEN SYMBOLS ARE DECREASING PULSES). RESPONSE = $\Delta EOT / \Delta EOT_{MAX}$	209
FIGURE 4-17 THE OPTICAL RESPONSE OF A PENTANOL-MODIFIED FABRY-PEROT POROUS SILICON SAMPLE DOSED WITH 2-HEXANOL VAPOUR. THE TOP GRAPH PLOTS THE EOT VS TIME FOR SPATIAL POSITION 3 (LABELS ON TOP OF EACH PULSE SHOW THE P/P_s VALUE FOR EACH PULSE). THE BOTTOM GRAPH PLOTS THE RESPONSE NORMALIZED TO THE VALUE OBTAINED AT THE HIGHEST CONCENTRATION VS P/P_s	

(CLOSED SYMBOLS ARE INCREASING PULSES AND OPEN SYMBOLS ARE DECREASING PULSES). RESPONSE = $\Delta EOT / \Delta EOT_{MAX}$	210
FIGURE 4-18 GRAPH OF THE OPTICAL RESPONSE TO ETHANOL VAPOUR, NORMALIZED TO THE VALUE OBTAINED AT THE HIGHEST CONCENTRATION VS P/P_s FOR ALL UNIFORMLY MODIFIED FABRY-PEROT POROUS SILICON SAMPLES. DATA REPRESENTS AVERAGES OF REPLICATE MEASUREMENTS AND THE ERROR BARS REPRESENT THE STANDARD DEVIATION. RESPONSE = $\Delta EOT / \Delta EOT_{MAX}$	212
FIGURE 4-19 GRAPH OF THE OPTICAL RESPONSE TO HEPTANE VAPOUR NORMALIZED TO THE VALUE OBTAINED AT THE HIGHEST CONCENTRATION VS P/P_s FOR ALL UNIFORMLY MODIFIED FABRY-PEROT POROUS SILICON SAMPLES. DATA REPRESENTS AVERAGES OF REPLICATE MEASUREMENTS AND THE ERROR BARS REPRESENT THE STANDARD DEVIATION. RESPONSE = $\Delta EOT / \Delta EOT_{MAX}$	213
FIGURE 4-20 GRAPH OF THE OPTICAL RESPONSE TO TOLUENE VAPOUR NORMALIZED TO THE VALUE OBTAINED AT THE HIGHEST CONCENTRATION VS P/P_s FOR ALL UNIFORMLY MODIFIED FABRY-PEROT POROUS SILICON SAMPLES. DATA REPRESENTS AVERAGES OF REPLICATE MEASUREMENTS AND THE ERROR BARS REPRESENT THE STANDARD DEVIATION. RESPONSE = $\Delta EOT / \Delta EOT_{MAX}$	214
FIGURE 4-21 GRAPH OF THE OPTICAL RESPONSE TO 2-HEXANOL VAPOUR NORMALIZED TO THE VALUE OBTAINED AT THE HIGHEST CONCENTRATION VS P/P_s FOR ALL UNIFORMLY MODIFIED FABRY-PEROT POROUS SILICON SAMPLES. DATA REPRESENTS AVERAGES OF REPLICATE MEASUREMENTS AND THE ERROR BARS REPRESENT THE STANDARD DEVIATION. RESPONSE = $\Delta EOT / \Delta EOT_{MAX}$	215
FIGURE 4-22 THE OPTICAL RESPONSE OF A PENTYL ACETATE GRADIENT MODIFIED FABRY-PEROT POROUS SILICON SAMPLE DOSED WITH HEPTANE VAPOUR. THE TOP GRAPH PLOTS THE EOT VS TIME FOR SPATIAL POSITION 4 (LABELS ON TOP OF EACH PULSE SHOW THE P/P_s VALUE FOR EACH PULSE). THE BOTTOM GRAPH PLOTS THE RESPONSE NORMALIZED TO THE VALUE OBTAINED AT THE HIGHEST CONCENTRATION VS P/P_s FOR ALL FOUR POSITIONS ALONG THE GRADIENT (CLOSED SYMBOLS ARE INCREASING PULSES AND OPEN SYMBOLS ARE DECREASING PULSES). RESPONSE = $\Delta EOT / \Delta EOT_{MAX}$	219
FIGURE 4-23 THE OPTICAL RESPONSE OF A PENTYL ACETATE GRADIENT MODIFIED FABRY-PEROT POROUS SILICON SAMPLE DOSED WITH TOLUENE VAPOUR. THE TOP GRAPH PLOTS THE EOT VS TIME FOR SPATIAL POSITION 3 (LABELS ON TOP OF EACH PULSE SHOW THE P/P_s VALUE FOR EACH PULSE). THE BOTTOM GRAPH PLOTS THE RESPONSE NORMALIZED TO THE VALUE OBTAINED AT THE HIGHEST CONCENTRATION VS P/P_s FOR ALL FOUR POSITIONS ALONG THE GRADIENT (CLOSED SYMBOLS ARE INCREASING PULSES AND OPEN SYMBOLS ARE DECREASING PULSES). RESPONSE = $\Delta EOT / \Delta EOT_{MAX}$	220
FIGURE 4-24 THE OPTICAL RESPONSE OF A PENTANOL GRADIENT MODIFIED FABRY-PEROT POROUS SILICON SAMPLE DOSED WITH ETHANOL VAPOUR. THE TOP GRAPH PLOTS THE EOT VS TIME FOR SPATIAL POSITION 2 (LABELS ON TOP OF EACH PULSE SHOW THE P/P_s VALUE FOR EACH PULSE). THE BOTTOM GRAPH PLOTS THE RESPONSE NORMALIZED TO THE VALUE OBTAINED AT THE HIGHEST CONCENTRATION VS P/P_s FOR ALL FOUR POSITIONS ALONG THE GRADIENT (CLOSED SYMBOLS ARE INCREASING PULSES AND OPEN SYMBOLS ARE DECREASING PULSES). RESPONSE = $\Delta EOT / \Delta EOT_{MAX}$	225
FIGURE 4-25 THE OPTICAL RESPONSE OF A PENTANOL GRADIENT MODIFIED FABRY-PEROT POROUS SILICON SAMPLE DOSED WITH HEPTANE VAPOUR. THE TOP GRAPH PLOTS THE EOT VS TIME FOR SPATIAL POSITION 2 (LABELS ON TOP OF EACH PULSE SHOW THE P/P_s VALUE FOR EACH PULSE). THE BOTTOM GRAPH PLOTS THE RESPONSE NORMALIZED TO THE VALUE OBTAINED AT THE HIGHEST CONCENTRATION VS P/P_s FOR ALL FOUR POSITIONS ALONG THE GRADIENT (CLOSED SYMBOLS ARE INCREASING PULSES AND OPEN SYMBOLS ARE DECREASING PULSES). RESPONSE = $\Delta EOT / \Delta EOT_{MAX}$	226
FIGURE 4-26 THE OPTICAL RESPONSE OF A PENTANOL GRADIENT MODIFIED FABRY-PEROT POROUS SILICON SAMPLE DOSED WITH TOLUENE VAPOUR. THE TOP GRAPH PLOTS THE EOT VS TIME FOR SPATIAL POSITION 2 (LABELS ON TOP OF EACH PULSE SHOW THE P/P_s VALUE FOR EACH PULSE). THE BOTTOM GRAPH PLOTS THE RESPONSE NORMALIZED TO THE VALUE OBTAINED AT THE HIGHEST CONCENTRATION VS P/P_s FOR ALL FOUR POSITIONS ALONG THE GRADIENTS (CLOSED SYMBOLS ARE INCREASING PULSES AND OPEN SYMBOLS ARE DECREASING PULSES). RESPONSE = $\Delta EOT / \Delta EOT_{MAX}$	227
FIGURE 4-27 THE OPTICAL RESPONSE OF A PENTANOL GRADIENT MODIFIED FABRY-PEROT POROUS SILICON SAMPLE DOSED WITH 2-HEXANOL VAPOUR. THE TOP GRAPH PLOTS THE EOT VS TIME FOR SPATIAL POSITION 2 (LABELS ON TOP OF EACH PULSE SHOW THE P/P_s VALUE FOR EACH PULSE). THE BOTTOM GRAPH PLOTS THE RESPONSE NORMALIZED TO THE VALUE OBTAINED AT THE HIGHEST CONCENTRATION VS P/P_s FOR ALL FOUR POSITIONS ALONG THE GRADIENT (CLOSED SYMBOLS ARE INCREASING PULSES AND OPEN SYMBOLS ARE DECREASING PULSES). RESPONSE = $\Delta EOT / \Delta EOT_{MAX}$	228

FIGURE 4-28 THE OPTICAL RESPONSE OF AN UNDECANOIC ACID GRADIENT MODIFIED RUGATE REFLECTOR POROUS SILICON SAMPLE DOSED WITH ETHANOL VAPOUR. THE GRAPH PLOTS THE RUGATE PEAK POSITION (Λ_{MAX}) VS TIME FOR SPATIAL POSITION 1 (LABELS ON TOP OF EACH PULSE SHOW THE P/P_s VALUE FOR EACH PULSE).	232
FIGURE 4-29 THE OPTICAL RESPONSE OF AN UNDECANOIC ACID GRADIENT MODIFIED RUGATE REFLECTOR POROUS SILICON SAMPLE DOSED WITH ETHANOL VAPOUR. THE TOP GRAPH PLOTS THE RUGATE PEAK POSITION (Λ_{MAX}) VS TIME FOR SPATIAL POSITION 2 (LABELS ON TOP OF EACH PULSE SHOW THE P/P_s VALUE FOR EACH PULSE). THE BOTTOM GRAPH PLOTS THE RESPONSE NORMALIZED TO THE VALUE OBTAINED AT THE HIGHEST CONCENTRATION VS P/P_s (CLOSED SYMBOLS ARE INCREASING PULSES AND OPEN SYMBOLS ARE DECREASING PULSES). RESPONSE = $\Delta\lambda / \Delta\lambda_{MAX}$	233
FIGURE 4-30 THE OPTICAL RESPONSE OF AN UNDECANOIC ACID GRADIENT MODIFIED RUGATE REFLECTOR POROUS SILICON SAMPLE DOSED WITH HEPTANE VAPOUR. THE GRAPH PLOTS THE RUGATE PEAK POSITION (Λ_{MAX}) VS TIME FOR SPATIAL POSITION 1 (LABELS ON TOP OF EACH PULSE SHOW THE P/P_s VALUE FOR EACH PULSE).	234
FIGURE 4-31 THE OPTICAL RESPONSE OF AN UNDECANOIC ACID GRADIENT MODIFIED RUGATE REFLECTOR POROUS SILICON SAMPLE DOSED WITH HEPTANE VAPOUR. THE TOP GRAPH PLOTS THE RUGATE PEAK POSITION (Λ_{MAX}) VS TIME FOR SPATIAL POSITION 2 (LABELS ON TOP OF EACH PULSE SHOW THE P/P_s VALUE FOR EACH PULSE). THE BOTTOM GRAPH PLOTS THE RESPONSE NORMALIZED TO THE VALUE OBTAINED AT THE HIGHEST CONCENTRATION VS P/P_s (CLOSED SYMBOLS ARE INCREASING PULSES AND OPEN SYMBOLS ARE DECREASING PULSES). RESPONSE = $\Delta\lambda / \Delta\lambda_{MAX}$	235
FIGURE 4-32 THE OPTICAL RESPONSE OF AN UNDECANOIC ACID GRADIENT MODIFIED RUGATE REFLECTOR POROUS SILICON SAMPLE DOSED WITH TOLUENE VAPOUR. THE GRAPH PLOTS THE RUGATE PEAK POSITION (Λ_{MAX}) VS TIME FOR SPATIAL POSITION 1 (LABELS ON TOP OF EACH PULSE SHOW THE P/P_s VALUE FOR EACH PULSE).	236
FIGURE 4-33 THE OPTICAL RESPONSE OF AN UNDECANOIC ACID GRADIENT MODIFIED RUGATE REFLECTOR POROUS SILICON SAMPLE DOSED WITH TOLUENE VAPOUR. THE TOP GRAPH PLOTS THE RUGATE PEAK POSITION (Λ_{MAX}) VS TIME FOR SPATIAL POSITION 2 (LABELS ON TOP OF EACH PULSE SHOW THE P/P_s VALUE FOR EACH PULSE). THE BOTTOM GRAPH PLOTS THE RESPONSE NORMALIZED TO THE VALUE OBTAINED AT THE HIGHEST CONCENTRATION VS P/P_s (CLOSED SYMBOLS ARE INCREASING PULSES AND OPEN SYMBOLS ARE DECREASING PULSES). RESPONSE = $\Delta\lambda / \Delta\lambda_{MAX}$	237
FIGURE 4-34 THE OPTICAL RESPONSE OF AN UNDECANOIC ACID GRADIENT MODIFIED RUGATE REFLECTOR POROUS SILICON SAMPLE DOSED WITH 2-HEXANOL VAPOUR. THE GRAPH PLOTS THE RUGATE PEAK POSITION (Λ_{MAX}) VS TIME FOR SPATIAL POSITION 1 (LABELS ON TOP OF EACH PULSE SHOW THE P/P_s VALUE FOR EACH PULSE).	238
FIGURE 4-35 THE OPTICAL RESPONSE OF AN UNDECANOIC ACID GRADIENT MODIFIED RUGATE REFLECTOR POROUS SILICON SAMPLE DOSED WITH 2-HEXANOL VAPOUR. THE TOP GRAPH PLOTS THE RUGATE PEAK POSITION (Λ_{MAX}) VS TIME FOR SPATIAL POSITION 2 (LABELS ON TOP OF EACH PULSE SHOW THE P/P_s VALUE FOR EACH PULSE). THE BOTTOM GRAPH PLOTS THE RESPONSE NORMALIZED TO THE VALUE OBTAINED AT THE HIGHEST CONCENTRATION VS P/P_s (CLOSED SYMBOLS ARE INCREASING PULSES AND OPEN SYMBOLS ARE DECREASING PULSES). RESPONSE = $\Delta\lambda / \Delta\lambda_{MAX}$	239
FIGURE 4-36 THE OPTICAL RESPONSE OF AN UNDECANOATE GRADIENT MODIFIED RUGATE REFLECTOR POROUS SILICON SAMPLE DOSED WITH ETHANOL VAPOUR. THE GRAPH PLOTS THE RUGATE PEAK POSITION (Λ_{MAX}) VS TIME FOR SPATIAL POSITION 1 (LABELS ON TOP OF EACH PULSE SHOW THE P/P_s VALUE FOR EACH PULSE).	242
FIGURE 4-37 THE OPTICAL RESPONSE OF AN UNDECANOATE GRADIENT MODIFIED RUGATE REFLECTOR POROUS SILICON SAMPLE DOSED WITH ETHANOL VAPOUR. THE TOP GRAPH PLOTS THE RUGATE PEAK POSITION (Λ_{MAX}) VS TIME FOR SPATIAL POSITION 2 (LABELS ON TOP OF EACH PULSE SHOW THE P/P_s VALUE FOR EACH PULSE). THE BOTTOM GRAPH PLOTS THE RESPONSE NORMALIZED TO THE VALUE OBTAINED AT THE HIGHEST CONCENTRATION VS P/P_s (CLOSED SYMBOLS ARE INCREASING PULSES AND OPEN SYMBOLS ARE DECREASING PULSES). RESPONSE = $\Delta\lambda / \Delta\lambda_{MAX}$	243
FIGURE 4-38 THE OPTICAL RESPONSE OF AN UNDECANOATE GRADIENT MODIFIED RUGATE REFLECTOR POROUS SILICON SAMPLE DOSED WITH WATER VAPOUR. THE GRAPH PLOTS THE RUGATE PEAK POSITION (Λ_{MAX}) VS TIME FOR SPATIAL POSITION 1 (LABELS ON TOP OF EACH PULSE SHOW THE P/P_s VALUE FOR EACH PULSE).	244
FIGURE 4-39 THE OPTICAL RESPONSE OF AN UNDECANOATE GRADIENT MODIFIED RUGATE REFLECTOR POROUS SILICON SAMPLE DOSED WITH WATER VAPOUR. THE TOP GRAPH PLOTS THE RUGATE PEAK	

POSITION (Λ_{MAX}) VS TIME FOR SPATIAL POSITION 2 (LABELS ON TOP OF EACH PULSE SHOW THE P/P_s VALUE FOR EACH PULSE). THE BOTTOM GRAPH PLOTS THE CHANGE IN RUGATE PEAK POSITION ($\Delta\Lambda_{\text{MAX}}$) VS P/P_s (CLOSED SYMBOLS ARE INCREASING PULSES AND OPEN SYMBOLS ARE DECREASING PULSES).	245
FIGURE 4-40 IMAGE OF THE UNDECANOIC ACID TO METHYL GRADIENT MODIFIED RUGATE REFLECTOR POROUS SILICON IMMERSSED IN WATER ( INDICATES THE DIRECTION OF THE GRADIENT FROM THE UNDECANOIC ACID END TO THE METHYL END. BOX SHOWS POSITION OF THE TRANSECT).	247
FIGURE 4-41 GRAPH OF THE MEDIAN GREEN AND BLUE PIXEL VALUES VS PIXEL POSITION ALONG THE TRANSECT OF AN UNDECANOIC ACID GRADIENT POROUS SILICON SAMPLE IMMERSSED IN WATER INDICATED IN FIGURE 4-40. INSERT ABOVE THE GRAPH SHOWS THE IMAGE OF THE TRANSECT.	248
FIGURE 4-42 SPECTRA SHOWING THE POSITION OF THE RUGATE PEAK WITH ETHANOL VAPOUR AT $P/P_s = 1.0$ AND WATER VAPOUR AT $P/P_s = 1.0$ AT POSITION 1 (UNDECANOATE END) FOR AN UNDECANOATE GRADIENT POROUS SILICON SAMPLE.	249
FIGURE 4-43 IMAGES OF THE POROUS SILICON SAMPLE WITH AN UNDECANOATE GRADIENT DOSED WITH (LEFT) $P/P_s = 1.0$ WATER VAPOUR AND (RIGHT) $P/P_s = 0.7$ ETHANOL VAPOUR ( INDICATES THE DIRECTION OF THE GRADIENT FROM THE UNDECANOATE END TO THE METHYL END).	250
FIGURE 4-45 RESPONSE OF AN RGB IMAGE DURING ETHANOL VAPOUR DOSING OF AN UNDECANOATE GRADIENT POROUS SILICON SAMPLE. TOP: GRAPH OF THE GREEN - BLUE PIXEL VALUES VS PIXEL POSITION ALONG THE TRANSECT. BOTTOM: GRAPH SHOWING CHANGE IN GREEN - BLUE PIXEL VALUES COMPARED TO $P/P_s = 0$ IMAGE VS PIXEL POSITION ALONG THE TRANSECT. VALUES IN LEGEND ARE P/P_s . ( INDICATES THE DIRECTION OF THE GRADIENT FROM THE UNDECANOATE END TO THE METHYL END).	252
FIGURE 4-46 TIME EVOLUTION OF THE RGB IMAGE RESPONSE UPON DOSING AT $P/P_s = 0.8$ ETHANOL VAPOUR ON AN UNDECANOATE GRADIENT POROUS SILICON SAMPLE. GRAPH SHOWS THE GREEN - BLUE PIXEL VALUES VS PIXEL POSITION ALONG THE TRANSECT. ( INDICATES THE DIRECTION OF THE GRADIENT FROM THE UNDECANOATE END TO THE METHYL END).	253
FIGURE 4-47 RGB IMAGE RESPONSE DURING WATER VAPOUR DOSING OF AN UNDECANOATE GRADIENT POROUS SILICON SAMPLE. TOP: GRAPH OF THE GREEN - BLUE PIXEL VALUES VS PIXEL POSITION ALONG THE TRANSECT. BOTTOM: GRAPH SHOWING THE CHANGE IN GREEN - BLUE PIXEL VALUES COMPARED TO $P/P_s = 0$ IMAGE VS PIXEL POSITION ALONG THE TRANSECT. VALUES IN LEGENDS ARE P/P_s . ( INDICATES THE DIRECTION OF THE GRADIENT FROM THE UNDECANOATE ACID END TO THE METHYL END).	255
FIGURE 4-48 TIME EVOLUTION OF RGB IMAGE RESPONSE DURING FOR DOSING AT $P/P_s = 1.0$ WATER VAPOUR OF AN UNDECANOATE GRADIENT POROUS SILICON SAMPLE. GRAPH SHOWS THE GREEN - BLUE PIXEL VALUES VS PIXEL POSITION ALONG THE TRANSECT. ( INDICATES THE DIRECTION OF THE GRADIENT FROM THE UNDECANOATE END TO THE METHYL END).	256
FIGURE 4-49 SINGLE POINT MEASUREMENTS OF THE CHANGE IN RUGATE PEAK POSITION UPON DOSING WITH WATER VAPOUR AT $P/P_s = 1.0$ OF AN UNDECANOATE GRADIENT POROUS SILICON SAMPLE. POSITION 1: THE UNDECANOATE END AND POSITION 2: THE METHYL END OF THE GRADIENT.	256
FIGURE 4-50 A DIFFERENCE IMAGE FOR GREEN AND BLUE CHANNELS OF AN RGB IMAGE AT $P/P_s = 0.8$ DOSING OF THE UNDECANOATE GRADIENT MODIFIED RUGATE REFLECTOR POROUS SILICON SHOWING STRIATIONS AND OTHER IMPERFECTIONS.	257
FIGURE 5-1 A LOGARITHMIC PLOT OF $\Delta EOT/EOT_{\text{INITIAL}}$ VS PARTIAL PRESSURE OF THE SOLVENT VAPOUR (PENTANOL MODIFIED FABRY PEROT POROUS SILICON).	270
FIGURE 5-2 TEMPORAL RESPONSE FOR DOSING OF AN UNDECANOIC ACID GRADIENT MODIFIED RUGATE REFLECTOR POROUS SILICON WITH 2-HEXANOL VAPOUR AT $P/P_s = 0.1$ (CA. 355 mL min^{-1} TOTAL GAS FLOW). INLET IS A HOLE ON THE RIGHT HAND SIDE OF IMAGES, WHILE OUTLET IS HOLE ON LEFT SIDE (BOTH APPROXIMATELY HALFWAY DOWN). THE IMAGES ARE THE DIFFERENCE BETWEEN THE GREEN CHANNEL OF A PHOTOGRAPH AT THE STATED TIME AND THE GREEN CHANNEL OF A PHOTOGRAPH TAKEN PRIOR TO DOSING, AND ARE CONTRAST ADJUSTED. ( INDICATES THE DIRECTION OF THE GRADIENT FROM THE UNDECANOIC ACID END TO THE METHYL END).	275

List of tables

TABLE 2-1 FLOW RATES FOR THE FLOW TUBE USED.	70
TABLE 2-2 PROCEDURE FOR PRECONDITIONING OF THE VAPOUR DOSING SETUP.	72
TABLE 2-3 FLOW RATES USED FOR DIFFERENT P/P_s FOR SOLVENT VAPOUR DOSING.	73
TABLE 2-4 GC-FID PARAMETERS.	74
TABLE 2-5 SATURATED VAPOUR CONCENTRATIONS AT $P/P_s = 1.00$ AT 20 °C.	75
TABLE 2-6 THE CONCENTRATIONS PREPARED FOR EACH SOLVENT.	75
TABLE 2-7 GC-FID RESULTS FOR ALL THE VAPOUR CONCENTRATIONS AT $P/P_s = 0.50$ AND THE SOLVENT VAPOUR SAMPLES USING VAPOUR DOSING SETUP 1.	76
TABLE 2-8 THE CALCULATED CORRECTION FACTORS FOR ALL OF THE SOLVENTS USING VAPOUR DOSING SETUP 1 AND THEIR ABSOLUTE ERRORS.	77
TABLE 2-9 ACTUAL P/P_s VALUES FOR EACH SOLVENT.	78
TABLE 3-1 TABLE OF FABRY-PEROT POROUS SILICON SAMPLES AND THEIR CALCULATED POROSITY WITH STANDARD ERROR AND THICKNESS.	88
TABLE 3-2 TABLE OF RUGATE SAMPLES AND THEIR CALCULATED POROSITY WITH STANDARD ERROR AND THICKNESS.	99
TABLE 4-1 PROPERTIES OF THE SOLVENTS USED FOR VAPOUR DOSING EXPERIMENTS. ²³¹	180
TABLE 4-2 BASELINE VALUES, EOT VALUES AT THE HIGHEST P/P_s AND THE OVERALL CHANGE IN EOT FOR A METHYLATED FABRY-PEROT POROUS SILICON SAMPLE BEING DOSED WITH VAPOURS FROM THE FOUR SOLVENTS. THE POROUS SILICON IS MONITORED AT THREE SPATIAL POSITIONS.	184
TABLE 4-3 BASELINE VALUES, EOT VALUES AT THE HIGHEST P/P_s AND THE OVERALL CHANGE IN EOT FOR A DECYL-MODIFIED FABRY-PEROT POROUS SILICON SAMPLE BEING DOSED WITH VAPOURS FROM THE FOUR SOLVENTS. THE POROUS SILICON IS MONITORED AT THREE SPATIAL POSITIONS.	192
TABLE 4-4 BASELINE VALUES, EOT VALUES AT THE HIGHEST P/P_s AND THE OVERALL CHANGE IN EOT FOR PENTYL ACETATE MODIFIED FABRY-PEROT POROUS SILICON SAMPLE BEING DOSED WITH VAPOURS FROM THE FOUR SOLVENTS. THE POROUS SILICON IS MONITORED AT THREE SPATIAL POSITIONS.	199
TABLE 4-5 BASELINE VALUES, EOT VALUES AT THE HIGHEST P/P_s AND THE OVERALL CHANGE IN EOT FOR A PENTANOL MODIFIED FABRY-PEROT POROUS SILICON SAMPLE BEING DOSED WITH VAPOURS FROM THE FOUR SOLVENTS. THE POROUS SILICON IS MONITORED AT THREE SPATIAL POSITIONS.	206
TABLE 4-6 TABLE OF THE DISTANCES FROM THE EDGE OF THE POROUS SILICON CLOSEST TO THE ASYMMETRIC ELECTRODE FOR THE FOUR SPATIAL POSITIONS AT WHICH THE EOT WAS MONITORED DURING DOSING.	216
TABLE 4-7 BASELINE VALUES, EOT VALUES AT THE HIGHEST P/P_s AND THE OVERALL CHANGE IN EOT AS MONITORED AT FOUR SPATIAL POSITIONS FOR A FABRY-PEROT POROUS SILICON SAMPLE WITH A PENTYL ACETATE COMPOSITIONAL GRADIENT BEING DOSED WITH HEPTANE OR TOLUENE.	218
TABLE 4-8 TABLE OF THE DISTANCES FROM THE EDGE OF THE POROUS SILICON CLOSEST TO THE ASYMMETRIC ELECTRODE FOR THE FOUR MONITORING POSITIONS USED FOR THE PENTANOL GRADIENT MODIFIED POROUS SILICON.	221
TABLE 4-9 BASELINE VALUES, EOT VALUES AT THE HIGHEST P/P_s AND THE OVERALL CHANGE IN EOT FOR FABRY-PEROT POROUS SILICON WITH A PENTANOL COMPOSITIONAL GRADIENT BEING DOSED WITH VAPOURS FROM THE FOUR SOLVENTS. THE POROUS SILICON IS MONITORED AT FOUR SPATIAL POSITIONS.	224
TABLE 4-10 BASELINE VALUES, RUGATE PEAK POSITIONS AT $P/P_s = 1.00$ AND THE OVERALL CHANGE IN RUGATE PEAK POSITION FOR RUGATE REFLECTOR POROUS SILICON WITH AN UNDECANOIC ACID COMPOSITIONAL GRADIENT BEING DOSED WITH ETHANOL VAPOUR WHILE BEING MONITORED AT TWO SPATIAL POSITIONS.	232
TABLE 4-11 BASELINE VALUES, RUGATE PEAK POSITIONS AT $P/P_s = 1.00$ AND THE OVERALL CHANGE IN RUGATE PEAK POSITION FOR RUGATE REFLECTOR POROUS SILICON WITH AN UNDECANOIC ACID COMPOSITIONAL GRADIENT BEING DOSED WITH HEPTANE VAPOUR WHILE BEING MONITORED AT TWO SPATIAL POSITIONS.	234

TABLE 4-12 BASELINE VALUES, RUGATE PEAK POSITIONS AT $P/P_s = 1.00$ AND THE OVERALL CHANGE IN RUGATE PEAK POSITION FOR RUGATE REFLECTOR POROUS SILICON WITH AN UNDECANOIC ACID COMPOSITIONAL GRADIENT BEING DOSED WITH TOLUENE VAPOUR WHILE BEING MONITORED AT TWO SPATIAL POSITIONS.	236
TABLE 4-13 BASELINE VALUES, RUGATE PEAK POSITIONS AT $P/P_s = 1.00$ AND THE OVERALL CHANGE IN RUGATE PEAK POSITION FOR RUGATE REFLECTOR POROUS SILICON WITH AN UNDECANOIC ACID COMPOSITIONAL GRADIENT BEING DOSED WITH 2-HEXANOL VAPOUR WHILE BEING MONITORED AT TWO SPATIAL POSITIONS.	238
TABLE 4-14 BASELINE VALUES, RUGATE PEAK POSITIONS AT $P/P_s = 1.00$ AND THE OVERALL CHANGE IN RUGATE PEAK POSITION FOR RUGATE REFLECTOR POROUS SILICON WITH AN UNDECANOATE COMPOSITIONAL GRADIENT BEING DOSED WITH ETHANOL VAPOUR WHILE BEING MONITORED AT TWO SPATIAL POSITIONS.	242
TABLE 4-15 BASELINE VALUES, RUGATE PEAK POSITIONS AT $P/P_s = 1.00$ AND THE OVERALL CHANGE IN RUGATE PEAK POSITION FOR RUGATE REFLECTOR POROUS SILICON WITH AN UNDECANOATE COMPOSITIONAL GRADIENT BEING DOSED WITH WATER WHILE BEING MONITORED AT TWO SPATIAL POSITIONS.	244
TABLE 5-1 WATER CONTACT ANGLES FOR ALL THE TERMINAL GROUPS ATTACHED TO POROUS SILICON IN THIS WORK.	266
TABLE 5-2 TABLE OF THE RATIO OF NORMALISED RESPONSE AT THE UNDECANOIC ACID OR UNDECANOATE END AND THE NORMALISED RESPONSE AT THE METHYL END OF THE GRADIENT FOR P/P_s VALUES BETWEEN 0.1 AND 0.8.	272

Abbreviations

AAS	Atomic absorption spectroscopy
AFM	Atomic force microscopy
ATR	Attenuated total reflectance
BBD	4-bromobenzenediazonium tetrafluoroborate
CCD	Charge coupled device
e^-	Electrons
EDAX	Energy dispersive X-ray spectroscopy
EDS	Energy dispersive spectroscopy
EOT	Effective optical thickness
FBD	3,4,5-trifluorobenzenediazonium tetrafluoroborate
FEG	Field emission gun
FFT	Fast Fourier Transform
FTIR	Fourier Transform infrared spectroscopy
FWHM	Full width at half maximum
GC-FID	Gas chromatograph – flame ionisation detector
GC-MS	Gas chromatograph – mass spectrometer
h^+	Holes
HF	Hydrofluoric acid
HPLC	High pressure liquid chromatography
IR	Infrared
LCTF	Liquid crystal tunable filter
MCT/A	Mercury Cadmium Telluride detector
NMR	Nuclear magnetic resonance spectroscopy
PDMS	Poly dimethylsiloxane
PID	Photoionisation detector
PL	Photoluminescence
ppm	Parts per million
PSi	Porous Silicon
RF	Radio frequency
RGB	Red green blue
SAM	Self assembled monolayer
SEM	Scanning electron microscopy
SIFT-MS	Selected ion flow tube mass spectrometer
SIMS	Secondary ion mass spectroscopy
STM	Scanning tunnelling microscopy
THF	Tetrahydrofuran
UV	Ultra violet
UV-Vis	Ultra violet – visible spectroscopy
VOCs	Volatile organic compounds
XPS	X-ray photoelectron spectroscopy